# BRIDGE RATING THROUGH NONDESTRUCTIVE LOAD TESTING

**NCHRP 12-28(13)A**

**TECHNICAL REPORT**

**A. G. Lichtenstein, P.E., Dr. Eng.**
**A. G. Lichtenstein and Associates, Inc.**
**Fair Lawn, New Jersey**

**June, 1993**

# CHAPTER 1

## INTRODUCTION

It is well known that a large percentage of our nation's bridges are structurally deficient and in need of posting and/or rehabilitation. Also, a significant number of bridges have hidden structural components and cannot be load rated analytically with any degree of confidence.

The results of bridge load tests have generally shown that many structures have greater load-carrying capacity than that predicted by calculations. Aside from the conservative approach used in design, the actual response of the structure under live load may be different due to the magnitude and distribution of loads, the interaction of structural (and to a lesser degree, non-structural) components, and the impact of deterioration and repairs.

The potential reduction in the number of bridges considered to be structurally deficient through the use of load testing was recognized in 1987 with the initiation of NCHRP Project 12-28(13), "Nondestructive Load Testing for Bridge Evaluation and Rating" (8). This project was completed in 1990. However, additional research was needed to develop a detailed procedure for integrating the results of load tests with rating calculations to establish the safe load capacity of bridges.

The primary goal of NCHRP Project 12-28(13)A, Bridge Rating Through Nondestructive Load Testing, was to develop a manual of procedures and techniques for incorporating bridge load test results into the bridge load rating process. Other objectives of this research included the development, presentation and refinement of a two-day workshop on bridge rating through load testing. To accomplish these objectives, a working plan consisting of eight tasks was developed and approved by TRB.

The major product of this project was the development of a "Manual for Bridge Rating Through Load Testing" which provides guidelines for integrating the load testing of bridges with their load rating.

The Manual includes recommendations based on the experience of the project team members in the load testing of bridges, published data on load tests and instrumentation and technical research conducted by project team members.

This report presents detailed data on two major technical areas: evaluating unintended composite action and establishing target proof load levels. The information contained in the next two chapters of this report was used as the basis for the guidelines and recommendations in the Manual. Each of these two chapters is independent of the other and stands alone, complete with equations and figures.

The material presented by Baidar Bakht in Chapter 2 is based on his own research, including field load tests, and has not been presented in its current form in any technical publication or conference. There are, however, other papers on unintended composite action which have been available to bridge engineers for review and comment (e.g. Ref. 7). The recommendations made by Bakht in Chapter 2 appear conservative with respect to findings reported by others (e.g. Ref. 7). The bridge owner should decide based on his own judgment and experience the applicability of the material presented in Chapter 2.

# CHAPTER 2

## EVALUATING COMPOSITE ACTION IN SLAB-ON-GIRDER BRIDGES WITHOUT MECHANICAL SHEAR CONNECTION BY BAIDAR BAKHT

### 2.1 INTRODUCTION

There are a great many of slab-on-girder bridges with concrete deck slabs and steel girders, or stringers, in North America which do not have any mechanical shear connection between the deck slab and the beams. It has been found through many field tests that despite the absence of mechanical shear connection, some composite action exists between the deck slab and the beams in most of these bridges. The composite action, which is believed to exist because of friction and bond between the steel and the concrete, however, is known to deteriorate with increase in load level. Bakht and Jaeger (2) have recommended that such composite action should be ignored completely in the strength calculation of the ultimate limit state.

It is emphasized that this recommendation of Bakht and Jaeger applies for only analytical evaluations. If full or partial composite action is confirmed by a proof test, then, of course, the composite action should be implicitly included in the evaluation of bridge strength. There is uncertainty, however, about the reliability of composite action found by a diagnostic test. The question is, can this composite action be assumed to exist at load levels higher than those of the diagnostic test?

The purpose of this chapter is to explore systematically the composite action in a slab and girder combination without mechanical shear connection, and to determine a procedure for extrapolating the results of diagnostic tests to give a bridge rating.

### 2.2 DETERIORATION OF COMPOSITE ACTION (WHEN NONE WAS INTENDED BY DESIGN)

Bakht and Jaeger (2) have provided evidence of the deterioration of the composite action with increasing load in structures which were designed as noncomposite. An example of the shifting of the neutral axis, indicating the changing degree of composite action, is presented in Fig. 1, which shows the strains at the top and bottom flanges of a stringer, plotted against the load level. The stringer belongs to the floor system of a truss bridge in which the floor beams are spaced at 14 ft centers, and in which there is no mechanical connection between the concrete deck slab and the stringers. The data for Fig. 1 have been taken from a report by Mahue and Agarwal (4).

In a slab-on-girder bridge, the neutral axis of the partially composite beams usually maintain their positions during the early stages of increasing loads. The neutral axis tends to move down at higher load levels, thus indicating the deterioration of the composite action. For the case shown in Fig. 1 the loss of the composite action was almost directly proportional to the load level.

It is important to note that the load-strain diagram shown in Fig. 1 was repeatable, i.e. unloading the bridge and then reloading resulted in similar strain patterns. This indicates that transfer of the horizontal shear from the stringer to the deck slab was an elastic phenomenon.

## 2.3 ELEMENTARY ANALYSIS

To study the mechanics of composite action, a simply supported beam carrying a uniformly distributed load with unit length is considered. The beam has a rectangular flange and a rectangular web both of concrete as shown in Fig. 2. To simplify calculations it is further assumed that the neutral axis of the composite beam lies in the web. This can be verified by using equation 9 below.

By considering a longitudinal segment of the beam of length dx (Fig. 2b), the shear force Q is obtained, as usual in terms of moment M.

$$Q = \frac{dM}{dx} \tag{1}$$

Similarly:

$$w = -\frac{dQ}{dx} = -\frac{d^2M}{dx^2} \tag{2}$$

## 2.4 INTERFACE VERTICAL SHEAR STRESS

Using the notation shown in Fig. 2(a) and denoting I as the moment of inertia of the composite beam, the vertical shear stress $\tau$ in the web at a distance z from the bottom (Fig. 3(a)) is given by:

$$\tau = \frac{Q(b_2 Z)(d_1 + d_2 - \bar{y} - 0.5Z)}{b_2 I} \tag{3}$$

The total shear force F taken by the web is obtained from

$$F = \frac{Q\,b_2}{I}\int_0^{d_2} z(d_1 + d_2 - \bar{y} - 0.5z)dz$$

or

$$F = \frac{Qb_2}{I}\left\{(d_1 + d_2 - \bar{y})\frac{d_2^2}{2} - \frac{d_2^3}{6}\right\} \tag{4}$$

The vertical interaction force per unit length between the flange and the web is denoted as $p_v$, as illustrated in Fig. 3(b). It is obvious that

$$p_v = -\frac{dF}{dx}$$

or using Eq. (4)

$$p_v = -\frac{b_2}{I}\left\{(d_1 + d_2 - y)\frac{d_2^2}{2} - \frac{d_2^3}{6}\right\}\frac{dQ}{dx}$$

Using Eq. (2), the above equation becomes

$$p_v = \frac{wb_2}{I}\left\{(d_1 + d_2 - \bar{y})\frac{d_2^2}{2} - \frac{d_2^3}{6}\right\} \tag{5}$$

## 2.5 INTERFACE HORIZONTAL SHEAR STRESS

The horizontal interactive shear force per unit length between the flange and the web is denoted as $p_h$. Using the familiar elementary theory, it can be shown that for any loading

$$p_h = \frac{Qb_1d_1(\bar{y} - 0.5\,d_1)}{I} \tag{6}$$

## 2.6 COMPOSITE ACTION THROUGH ONLY FRICTION

If the composite action takes place only through friction between the web and the flange, then it is obvious that

$$p_h \leq \mu\, p_v \tag{7}$$

Where $\mu$ is the coefficient of Coulomb friction. Using Eqs. (5) and (6), relationship (7) can be written as:

$$Q\,b_1d_1(\bar{y} - 0.5d_1) \leq \mu\, w\, b_2\left\{(d_1 + d_2 - \bar{y})\frac{d_2^2}{2} - \frac{d_2^3}{6}\right\} \tag{8}$$

It is recalled that $\bar{y}$ is given by:

$$\bar{y} = \frac{b_1 d_1^2 + b_2 d_2^2 + 2 b_2 d_1 d_2}{2\left(b_1 d_1 + b_2 d_2\right)} \tag{9}$$

For a simply supported beam of span L and carrying a uniformly distributed load, w, per unit length, Q = 0.5 wL. By substituting this expression for Q in inequality (8), it can be appreciated the w occurring on both sides is self canceling. Consequently, for a given cross section, L and m are the only variables which determine whether the full composite action can be developed by friction alone. The limiting value of L obtained from inequality (8) is given as follows:

$$L \le \frac{2\mu b_2 \left\{ \left(d_1 + d_2 - \bar{y}\right) \frac{d_2^2}{2} - \frac{d_2^3}{6} \right\}}{b_1 d_1 \left(\bar{y} - 0.5 d_1\right)} \tag{10A}$$

Figure 4 shows the cross section of an equivalent beam in which for ease of calculation, both the flange and the web are assumed to be of the same material. For this cross section using $\mu = 1.0$, the limiting value of L is found to be 49.1 inches. Clearly, this very small limiting span length indicates that friction alone is not very effective in generating the composite action.

## 2.7 EXAMPLE

To explore qualitatively the effect of friction on the composite action, an example is presented. The example is that of the most heavily loaded girder of the slab-on-girder bridge tested to failure by Bakht and Jaeger (2). The cross section of the girder and the associated portion of the deck slab is shown in Fig. 5(a). For a modular ratio of 10, the effective moment of inertia of the fully composite section is found to be 5336 $in^4$ in steel units. The effective applied loading on one girder is shown in Fig. 5(b). As shown by Jaeger and Bakht (3), this partial uniformly distributed load can be represented approximately by a sinusoidally distributed load of intensity $p_x$ which is given by:

$$p_x = \frac{2P}{\pi u} \sin \frac{\pi u}{L} \sin \frac{\pi x}{L} \tag{10B}$$

Where u is half the length of the centrally-placed load P, x is the distance along the beam from the left support, and L is the span. It can be shown that for the loading shown in Fig. 5(b), $p_x$ is given by:

$$p_x = 0.05625 \sin \frac{\pi x}{540} \tag{11}$$

In this expression, x is in inches and $p_x$ in kips/in. (See Fig. 5(c)).

To obtain the maximum benefit of friction, it is assumed that (a) $\mu = 1.0$; (b) all the applied loading is transferred through the deck slab and girder interface as $p_v$; and (c) the dead load of the deck slab, etc. is of the same order of magnitude as the live load. In this case, the friction force $p_u = 2 \times \mu \times p_x$ or:

$$p_u = 0.1125 \sin \frac{\pi x}{540} \text{ (kips/in)} \tag{12}$$

It can be shown that shear $Q_x$ along the span is given by:

$$Q_x = \frac{2PL}{\pi^2 u} \sin \frac{\pi u}{L} \cos \frac{\pi x}{L} \tag{13}$$

Replacing Q in Eq. (6) by $Q_x$, the expression for $p_h$ becomes:

$$p_h = 3.529 \cos \frac{\pi x}{540} \text{ (kips/in)} \tag{14}$$

The quantitative comparison of $p_u$ and $p_h$ thus obtained is presented in Fig. 6 for the entire length of the beam. It can be seen in this figure that (a) the resistance that can be generated by friction is very small compared to the horizontal interface shear; and (b) the patterns of the interface horizontal shear and the corresponding frictional resistance are not compatible to each other, so that, for example at the supports the former attains the highest value and the latter the lowest. It is also worth noting that in practice, $p_u$ is likely to be smaller than the values given by Eq. (12), in which case the contribution of friction to the composite action would be even smaller.

## 2.8 CONCLUSION WITH RESPECT TO FRICTION

From the above discussion, it is obvious that friction is not significantly effective in generating the composite action between a beam and the deck slab. Any composite action observed in the absence of mechanical shear connection should be attributed to factors other than friction. If friction had a significant influence, the composite action would have been observed in all girders, and this is clearly not the case.

## 2.9 COMPOSITE ACTION THROUGH ONLY BOND

The term "bond" is used herein for the chemical bond between the concrete of the deck slab and the flange of the steel girder; it is also used for the resistance that may be generated due to aggregate interlocking between the concrete of the deck slab and a delaminated strip of concrete that has detached from the deck slab but is still bonded to the flange of the girder. Unlike resistance due to friction, both these kinds of resistance are believed to be relatively free from the normal pressure at the interface.

Unfortunately, except for a field test, there is no practical way of ascertaining if bond exists between the deck slab and girders. It has been observed that when the top flange of girder is partially embedded in the deck slab, the bond resistance is very effective in promoting the composite action. However, even this generally true statement is not free from exceptions. In the bridge tested by Bakht and Jaeger (2) to failure, it was observed that despite their top flanges being partially embedded in the deck slab, the two outer girders had practically no composite action even at low levels of loads.

If in the absence of mechanical shear connection, the presence of the composite action is confirmed by a proof test, then clearly it can be relied upon for the nominal ultimate evaluation load. Such reliance on the composite action, however, may not be axiomatic if its presence is established only at low level loads of a diagnostic test.

To explore the degree of composite action beyond the level of the test load, the realistic case of the composite beam shown in Fig. 5(a) is considered. The moment of inertia of the non-composite slab and beam combination is 2169 $in^4$ (steel units) and that of the fully composite beam 5336 $in^4$ (also in steel units). The beam is subjected to gradually increasing load.

It is assumed that during the initial stages of loading the bond between the concrete deck slab and the steel beam remains intact thereby offering full composite action. The load-deflection curve for the fully composite beam is shown schematically in Fig. 7 by line OA. If the bond between the concrete and steel breaks completely at load level A, the deflection of the beam will suddenly increase by a factor of 5336/2169 (=2.46), in which case the deflection will increase from A to B. For higher loads, the load deflection curve would follow BC. If the breakage of the bond is permanent, the load-deflection curve for subsequent loading will be similar to OBC.

In practice, the deflections of slab-on-girder bridges without mechanical shear connection do not suddenly increase under gradually increasing loads. In most cases, the load-deflection curves of these bridges are linear in the initial stages of the load, thus following the path OA in Fig. 7. The curves become nonlinear similar to path AD under heavier loads. Unless the steel of the girder has yielded, upon removal of the load all the deflections are recovered with the load-deflection curve following path DEO.

The typical observed load-deflection curve presented in Fig. 7 confirms that

a. the bond strength, while deteriorating with increasing load, does not suddenly drop to zero;

b. the deterioration of the bond strength under high load levels is not permanent, i.e. the bond strength can be relied upon even if the limit of linearity is exceeded.

In the light of the above discussion, it seems feasible to divide the load-deflection behavior of the beam and slab combination into two linear segments, OA and AF shown in Fig. 7. In segment OA, the deck slab acts compositely with the steel beam. The upper limit of this segment is defined by the load which causes the interface horizontal shear to reach the limiting, and pre-specified, bond stress.

Segment AF represents the behavior when the slab and the beam flex about their own respective neutral axes, i.e. when the section acts non-compositely.

Figures 8(a) and (b) show a schematic representation of the process of extrapolating the level of proof load from the results of diagnostic testing. The former figure shows the case in which the load of the diagnostic test causes smaller interface horizontal shear stress than the limiting bond stress. In such a case, the diagnostic test is useful in only establishing the presence of bond between the deck slab and the girders. The finding of the proof load by extrapolation is done by using the bilinear load deflection behavior described above.

When the diagnostic test loads are high enough to cause higher interface horizontal shear than the limiting bond stress, then as shown in Fig. 8(b), the test load should be regarded as the limiting load beyond which the section ceases to act compositely.

## 2.10 SUGGESTED BOND STRENGTHS

Agarwal and Selvadurai (1) have suggested that a conservative value of bond strength between the concrete deck slab and steel girders can be assumed to be $0.1\sqrt{f'_c}$, where the compressive strength of concrete, $f'_c$, is in MPa. For 3000 psi concrete, this bond strength is about 70 psi.

It is suggested that in the absence of more reliable information, this bond strength be used for those bridges in which the deck slab rests above the girder flanges. Where the top flanges of the girders are partially, or fully, embedded in the deck slab, the bond strength is expected to be much higher; 100 psi is recommended.

It is emphasized that these values of bond stresses should be used only after the girder strains obtained during the diagnostic test have confirmed that the neutral axis of the section is high enough to justify the assumption of composite action.

The values of bond strengths recommended above are on the conservative side. Bond strengths of up to 145 psi have been observed (Agarwal and Selvadurai (1)).

## 2.11 ILLUSTRATIVE EXAMPLE

To illustrate the proposed technique, a slightly modified form of the bridge tested to failure by Bakht and Jaeger (2) is selected as an example with one layer of blocks being regarded as the diagnostic loading. The cross section of the girder and the associated portion of the deck slab receiving the maximum share of the test load are shown in Fig. 5(a). The following are assumed:

a. The girder attracts about one third of the total test load of 48 kips; i.e. 16 kips, is shown in Fig. 5(b).

b. The yield stress of the girder steel is 30 ksi and the maximum dead load stress in the girder is 7.2 ksi leaving 22.8 ksi stress or $760 \times 10^{-6}$ in/in strain available for the test load ($E = 30 \times 10^6$ psi).

c. The extrapolated proof test load, will be the calculated load which causes a maximum strain of $760 \times 10^{-6}$ in/in in the girder under consideration.

d. The bearing restraint offers negligible resistance to the movement of the girders.

e. Under diagnostic loading, the girder at the mid-span was found to have -21 and 200 x $10^{-6}$ in/in strains in the top and bottom flanges, respectively.

If the composite action between the deck slab and the girder is ensured by adequate mechanical shear connectors, the extrapolated proof load would simply be (760/200) x 48 = 182 kips. In the absence of such shear connectors, the steps in Sections 2.12 through 2.15 would have to be taken to obtain the extrapolated proof load.

## 2.12 CALCULATION OF INTERFACE HORIZONTAL SHEAR

The maximum shear due to the diagnostic load is 8 kips. Therefore, the maximum interface horizontal shear, $p_h$ is given by Eqn. 6:

$$p_h = \frac{(8000)48(7)\left(9.3 - 0.5(7)\right)}{(10)(5336)}$$

$$p_h = 292 \text{ psi}$$

Since the width of the girder flange is 9 in., the interface horizontal shear stress = 292/9 = 32 psi.

## 2.13 CALCULATION OF LOAD CAUSING LIMITING INTERFACE SHEAR

The permissible bond strength for the embedded flange, as given earlier, is 100 psi. Consequently, the load causing the limiting interface horizontal shear stress = (100/32) x 48 = 150 kips. The maximum tensile strain caused by this load is (150/48) x 200 = 625 x $10^{-6}$ in/in, so that strain of (760-625) = 135 x $10^{-6}$ in/in is available for further loading under which the girder will be assumed to be noncomposite.

## 2.14 CALCULATION OF REMAINING LOAD CAPACITY

As discussed earlier, after the limiting bond stress has been exceeded, the girder will be assumed to be acting noncompositely. For simplicity, it is further assumed that the girder will sustain all the load.

The moment of inertia of the 24-in-deep steel girder is 2032 $\text{in}^4$. The maximum moment due to the 16 kip load on the beam (Fig. 5b), or the total test load of 48 kips, is 1776 kip-in. The maximum stress caused by this moment in the naked steel girder = 1776 x 12/2032 = 10.5 ksi. This stress is equivalent to 350 x $10^{-6}$ in/in strain. The total load causing the maximum strain of 135 x $10^{-6}$ in/in = (135/350) x 48 = 18.5 kips.

## 2.15 EXTRAPOLATED PROOF LOAD

From the above calculations, the total extrapolated proof load = 150+18.5 = 168.5 kips, which is only about 7% less than the proof load which is obtained by assuming that the degree of composite action found in the diagnostic test will hold at the level of the proof load.

If the bond strength was assumed to be effective only up to the level of the diagnostic test, the proof load would have dropped to about 142 kips based on noncomposite action for loading beyond the level of the test loads.

## 2.16 CONCLUSIONS

It has been demonstrated that any composite action that might exist in slab-on-girder bridges without mechanical shear connections, is predominantly due to bond between the deck slab and the girders. An analytical method has been provided for obtaining the value of the proof loads from the results of a diagnostic test on a slab-on-girder bridge.

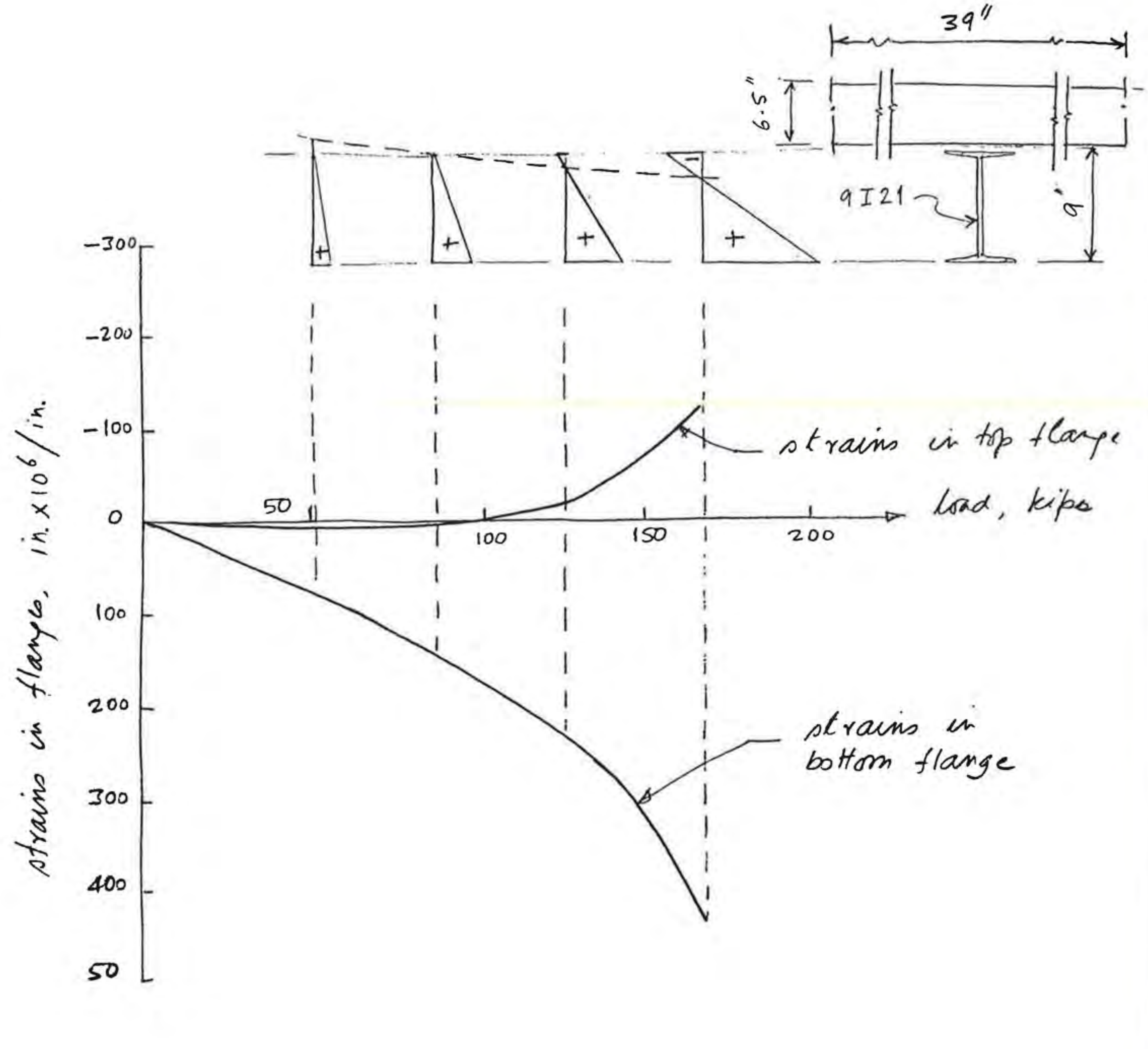


FIGURE 1: Observed strains in stringer of truss bridge

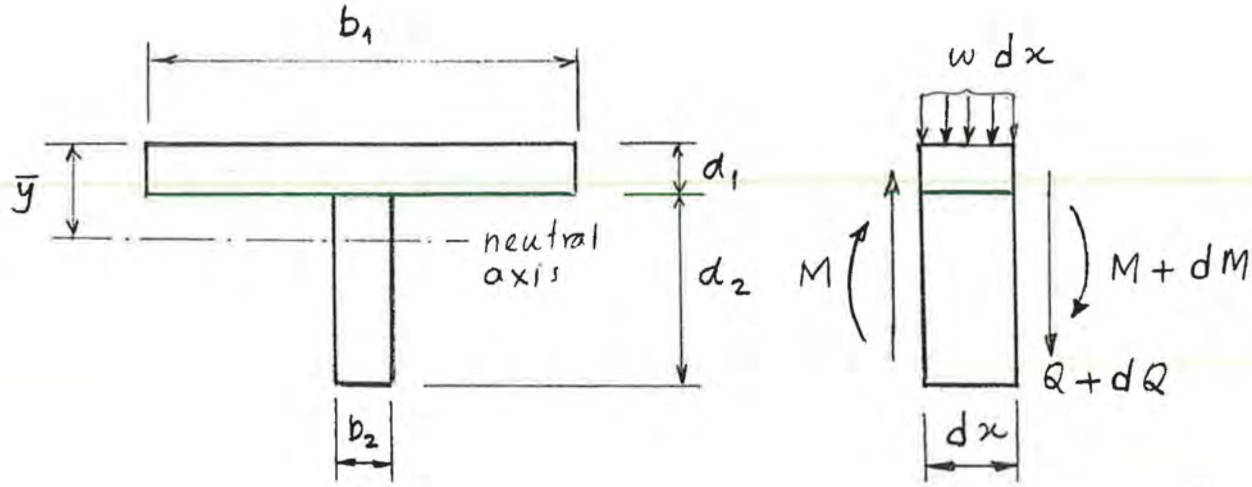


(a) Cross-section

(b) Longitudinal Segment

FIGURE 2: Concrete Composite Beam

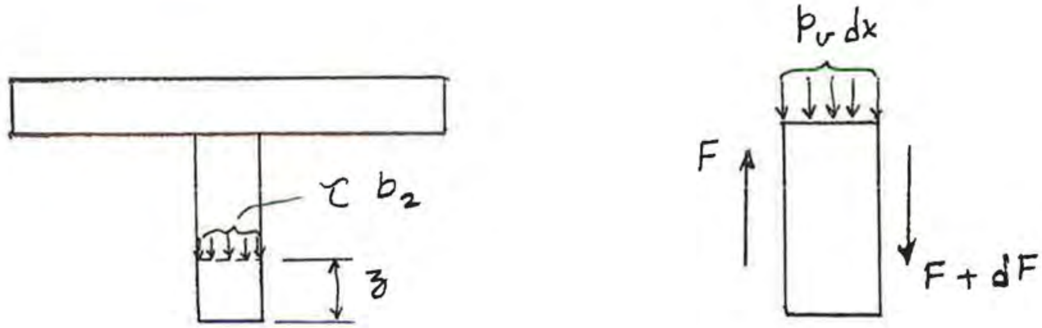


(a) Cross-Section

(b) Longitudinal Segment of Girder Only

FIGURE 3: Shear Stress

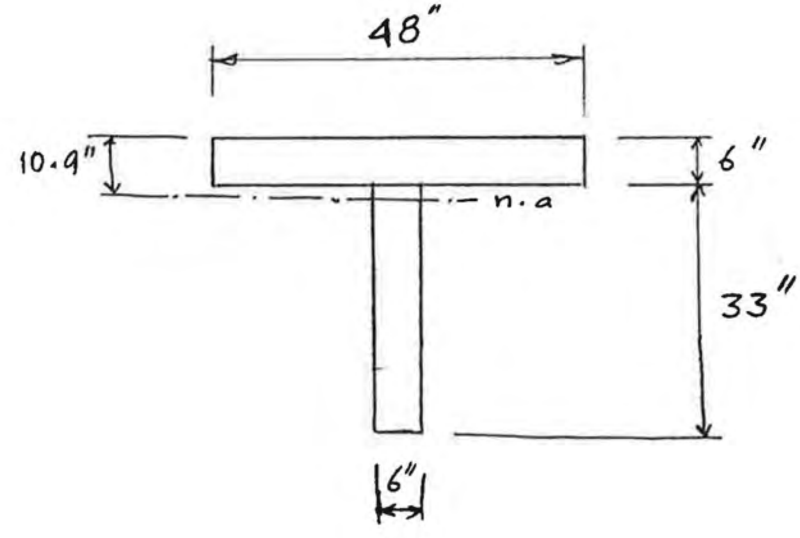


FIGURE 4: Cross Section of Concrete Composite Beam

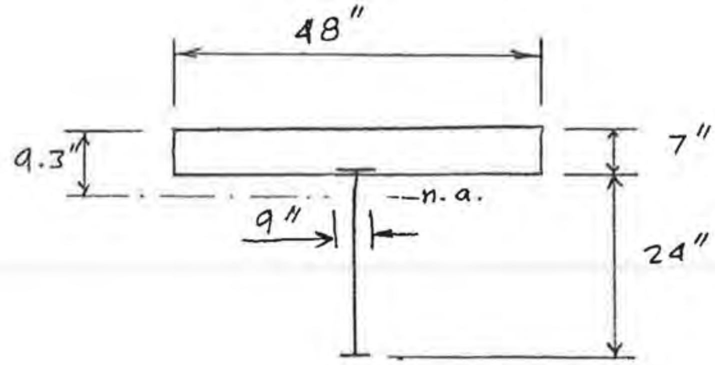


(a) Cross Section of Steel-Concrete Composite Beam

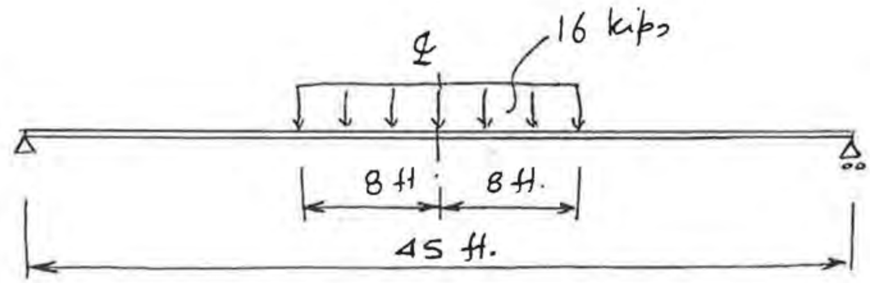


(b) Loading on Beam

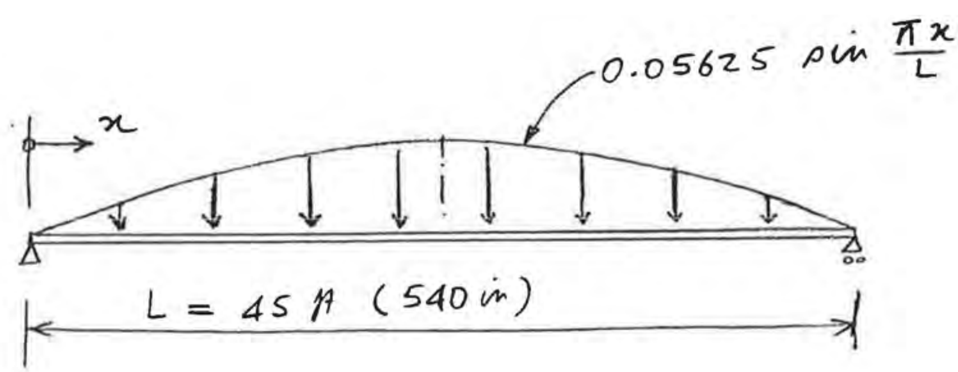


(c) Equivalent Loading

FIGURE 5: Composite Beam and Loading

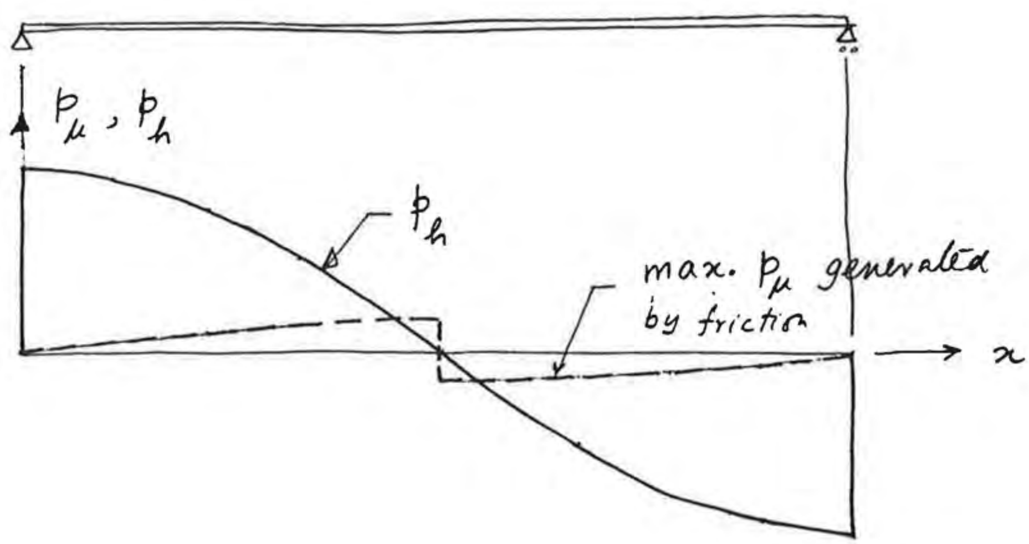


FIGURE 6: Comparison of Interface Horizontal Shear ($p_h$) and Resistance Due to Friction ($p_\mu$)

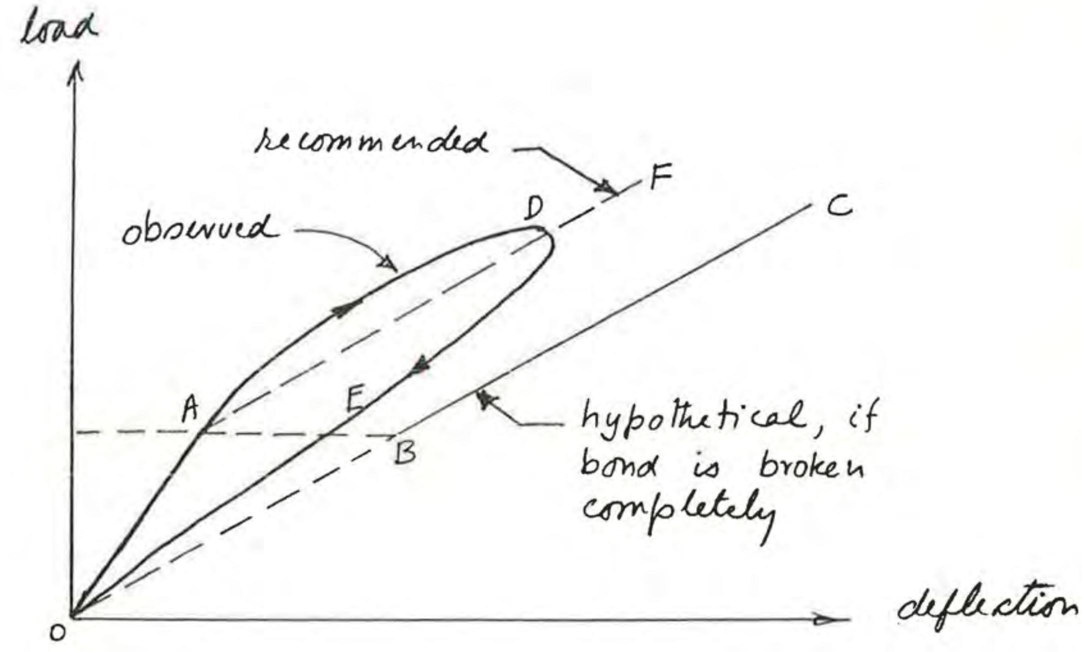


FIGURE 7: Load-Deflection Curves for Beam in which Composite Action Exists Due Only to Bond

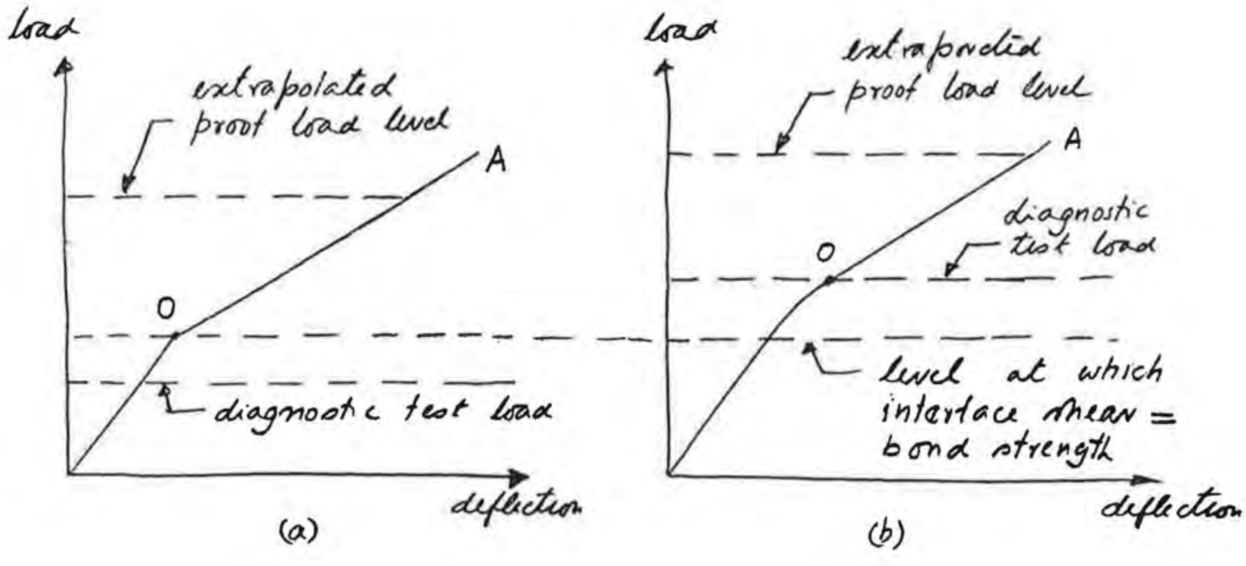


NOTE: For OA segment no composite action is assumed

FIGURE 8: Schematic Representation of Determining Extrapolated Proof Load Level

# CHAPTER 3

## DERIVATION OF PROOF LOADING FACTORS
## BY FRED MOSES

### 3.1 SUMMARY

This chapter presents the basis for the recommended proof loading factors as outlined in Chapter 7 of the "Manual for Bridge Rating Through Load Testing." In particular, the different adjustments that may be needed to determine a target proof load are described herein. This material is presented as a background document to outline the methodology. It is not intended that individuals applying the recommendations in the Manual will have to consult this material in selecting a proof load factor. Rather, this chapter shows the technical basis for the recommended factors. As greater use is made of load and resistance factors following future adoption of AASHTO LRFD design and evaluation procedures, further review may be needed to provide more uniformity in safety between the various design, evaluation and testing procedures.

### 3.2 BACKGROUND

The derivation of proof-test load factors is based on several premises related to bridge safety. Following a proof test, a bridge which is opened to normal traffic should provide the same level of safety as a bridge which is checked by conventional analysis and rating methods. The higher confidence in the performance that results from a proof test will be reflected in permitting lower safety margins and/or less conservative assumptions about behavior and strength compared to those values used in a "paper" verification of bridge capacity.

Among the major uncertainties given in the AASHTO Manual for Condition Evaluation of Bridges (C/E Manual), which requires concern for safety, is the possibility of future overloading of the bridge and the possible development of further deterioration beyond that observed during the inspection. These uncertainties remain regardless of the fact that a proof test was carried out and are incorporated in the derivation of the proof load factors.

### 3.3 SAFETY MODELING

At present, the AASHTO C/E Manual provides a range of safety factors for capacity rating which can lead at their extreme limits to operating and inventory levels. States are then free to select either extreme value or some other level for the determination of posting loads. Different capacities for inventory and operating will also depend on whether working stress or load factor methods of checking are used. The Inventory levels are comparable to the current design safety factor and the Operating level was arbitrarily arrived at to ensure that typical H15 bridges will still be acceptable with current loadings.

The newly developed AASHTO LRFD specifications are different from the present design or inventory safety checks. The safety factors in the LRFD were derived to better correspond to modern truck loads and traffic and to provide more uniform safety over the full range of bridge spans, geometries and materials. Safety in the LRFD format is controlled in terms of a safety index ($\beta$), which accounts for various uncertainties in material properties, bridge behavior, loads and load analysis.

The LRFD framework is suitable for deriving the load factors needed for a proof test. This derivation can incorporate the level of proof testing and the added information obtained from a successful test. Further, the LRFD procedure is used to give the adjustments in the load factor for various circumstances described in the test manual, such as fracture critical members, site loading and inspection intervals.

One limitation in the LRFD procedures is the limited database for assigning statistical parameters needed to calculate the safety index. Further, there is the important issue of the target safety index that should be present after a bridge capacity assessment. These difficulties are alleviated by calibration of the proof-load factors to the safety targets implicit in the new AASHTO LRFD design and evaluation specifications. Also, the statistical data used in those derivations are assumed to be applicable to the present analysis as well as the implicit target betas. It can be seen from a sensitivity study that the derived proof-load test values are not very sensitive to any fluctuations in these parameters as long as the full calibration process is considered. That is, if a given proof load provides the target safety index comparable to the LRFD specifications with corresponding database, then the same proof load will be adequate if a change is made in the statistical database.

## 3.4 CALIBRATION OF SAFETY INDICES

For simplicity, the safety index will be shown in the following so-called "normal" format. That is, assuming that load and resistance are normal distributions, the safety index $\beta$ can be expressed as:

$$\beta = \frac{\text{Mean margin of safety}}{\text{Standard deviation of safety margin}} \qquad (1)$$

An exact expression for the probability of failure can be had by using a normal probability table, available in any statistics book. Thus, $\beta = 3$ corresponds to a failure probability of about $10^{-3}$. Similarly, risks can be found for other values of $\beta$. To avoid dealing explicitly with risk numbers, however, structural codes usually express risk directly in terms of $\beta$. For example, in the AISC code, betas of 3.5 for main members and 4.5 for connections are given as target values. If load and resistance follow standard normal distributions, then these risk values are precise; otherwise, these are only approximate.

Letting the margin of safety be written as g, we have:

$$g = \text{Resistance (strength)} - \text{Load Effect} \qquad (2)$$

or in typical terminology,

$$g = R - S \tag{3}$$

where the Mean is

$$\bar{g} = \bar{R} - \bar{S} \tag{4}$$

and

$$\sigma_g = \sqrt{\sigma_R^2 + \sigma_S^2} \tag{5}$$

Alternatively, the influence of the safety factor can be seen by rewriting Eqn. 4 as:

$$g' \frac{\bar{R}}{\bar{S}} - 1 = n - 1 \tag{6}$$

where n is the safety factor and g' is the margin of safety, referenced to the mean load and mean strength rather than the nominal values usually considered.

The final definitions relate to the expressions of statistical scatter in terms of the nondimensional coefficient of variation COV, (or $V_x$) which is defined as:

$$\mathrm{COV} = \frac{\text{Standard deviation}}{\text{Mean value}} \tag{7}$$

Since engineers usually use conservative values for their variables in code checking, a bias is introduced which is defined as:

$$\mathrm{BIAS} = \frac{\text{Mean value}}{\text{Nominal code value}} \tag{8}$$

The remaining part of this section introduces the database appropriate for calculating the safety indices. In general, these are values assigned by the various code committees and do not involve the designers. The latter see only the end product which is the safety factors calibrated by the code committees to achieve the appropriate safety indices.

Resistance—For many materials and representative component limit states the COV of resistance ranges close to 0.10. In addition, due to material specifications, the mean value of material strength is about 12% above the nominal value, i.e. $BIAS_R$ = 1.12. For example, the mean yield strength of A36 steel is about 42 ksi.

Load—The total load effect Q can be written as:

$$Q = D + L + I \tag{9}$$

where, D, L, and I are the dead, live and impact load effects, respectively.

The mean and sigma of the total load are then:

$$\bar{Q} = \bar{D} + \bar{L} + \bar{I} \tag{10}$$

$$\sigma_Q = \sqrt{\sigma_D^2 + \sigma_L^2 + \sigma_I^2} \tag{11}$$

Dead Load—This quantity will vary depending on whether asphalt overlay makes up a significant part of the dead load or whether most of the dead load is the steel and concrete of the beams and deck. Typically, the following parameters apply:

$$BIAS_D = 1.0, \text{ and } V_D = 0.10$$

Live Load—The data for live loads is taken from material developed by Nowak for the AASHTO LRFD bridge design specifications. Although the database for live load is limited by the sites available to that study, the reasoning is consistent and their use here should lead to proof-load factors consistent with the new LRFD safety criteria. For typical span ranges, the Nowak study shows a mean maximum load per lane over a lifetime (75 year) exposure of 1.79 x AASHTO HS20 loading. That is, it is expected that on the average the lane load will reach 1.79 HS20 vehicles in a single lane. For the combined two-lane loading case, the load is reduced to 0.85 x the one-lane situation. That is, simultaneously, once per 75 years both lanes are expected to see, on the average, 0.85 x 1.79 AASHTO loads in each lane. The COV for this live load is given by Nowak as 0.18. These COV cover both the uncertainty of heavy truck occurrences and the uncertainty associated with estimating the effects of these trucks on particular members of the structure (analysis COV). If only the truck load uncertainty and not the analysis is considered, the 0.18 COV should be reduced to about 0.14 based on Nowak's report.

Impact—Dynamic allowances are represented as a percentage of the live load, independent of span length. Nowak reports the mean impact as 10% with a large scatter represented by a COV of 0.80.

## 3.5 CALIBRATION TARGETS

An important aspect of selection of safety margins in the LRFD format is the target safety index. Typically, these are selected by examining existing designs having satisfactory performance. Beta values are extracted from these designs to provide safety levels for the future code changes. Specifications are changed when it is observed that there are significantly varying safety indices for different designs, which need realignment by modifying the LRFD safety factors. The averages of many designs are typically used in selecting the target betas.

From the AASHTO LRFD studies, it has been determined that the target betas should be about 3.5 corresponding to inventory design levels. For the AASHTO Guide Specifications for the Strength Evaluation of Existing Steel and Concrete Bridges (Guide Specifications), the target beta of about 2.3 was found comparable to the operating levels of rating. These lower betas for rating are justified since they reflect past rating practices at the operating levels. For the purpose of posting levels, however, system considerations and member failure consequences are also introduced in the AASHTO Guide Specifications. For example, non-redundant members are assigned lower allowables to bring their safety index to design levels, namely 3.5. Similarly, members with significant deterioration, or for which poor maintenance and infrequent inspections are evident are also assigned lower allowables. These latter situations reflect greater uncertainties in estimating nominal strength or performance variables.

In the new AASHTO C/E Manual, the operating levels require a factor of 1.3 on the combined dead plus live load and impact in the load factor method and a factor of 1.33 in the working stress format. These factors cover all the uncertainties described above. During the proof test, the structure supports both the existing dead load plus whatever live load is applied. A successful proof test should achieve, not the same total load effect as the 1.3 or 1.33 evaluation factor just mentioned, but the same target level of reliability.

Following the proof test, uncertainties are eliminated on the dead load and the strength capacity to support an appropriate pattern of the live load effect. The major uncertainties still remaining after the proof test are the magnitude of future live loads (which may exceed the rating and/or the legal load) and possible future deterioration.

## 3.6 EXAMPLES

### 3.6.1 General

To illustrate the calculation of safety indices, an example will be given. Cases will be described of a design which satisfies the AASHTO Standard Specifications for Highway Bridges (Design Code) and for which no proof test has been performed. Also, results will be shown for cases where proof test have been done to improve ratings. Subsequently, a general presentation of the proof-load factors will be given.

### 3.6.2 Example 1 - No Test Has Been Performed

60 ft. simple span - two lanes

HS20 L.L. - 807 k-ft/Lane

Code Impact, $I = \frac{50}{60+125} = .27$ (=218 k-ft)

For this example assume D.L., same as AASHTO L.L., = 807 k-ft/lane

Inventory level strength (working stress method): The nominal resistance capacity, $R_n$, required per lane after considering lateral load distribution is:

$$R_n = 1.82\,(807+807+218) = 3334 \text{ k-ft}$$

Note: $1.82 = \frac{1}{0.55}$ where 0.55 is the Inventory level allowable stress factor.

Using Eqn. 8 gives for the resistance:

$$\text{Mean, } \overline{R} = 1.12\, R_n = 3734 \text{ k-ft}$$

$$\text{Standard Deviation } \sigma_R = V_R\, \overline{R} = 0.10(3734) = 373 \text{ kip-ft}$$

$$\text{Dead Load, Mean, } \overline{D} = \text{Nominal} = 807$$

$$\sigma_D = \overline{D} V_D = 807(0.10) = 80.7$$

From data given above for the Live Load statistics, the expected maximum load (average load per lane):

$$\overline{L} = 0.85\ (1.79)(807) = 1228 \text{ k-ft}$$

where 0.85 accounts for 2 lanes and 1.79 gives mean largest load for 75-year projection.

$$V_L = 0.18 \text{ (includes analysis uncertainty)}$$

$$\sigma_L = .18(1228) = 221$$

Impact, Mean $\bar{I} = 0.1\ (1228) = 122.8$ (i.e. mean impact value is only 10%)

$$\sigma_I = .8\ (122.8) = 98$$

from Eqn. 9 the Total Load Q = D+L+I

Mean, $\overline{Q} = 807 + 1228 + 122.8 = 2157.8$

Standard Deviation, $\sigma_Q = \left[80.7^2 + 221^2 + 98^2\right]^{\frac{1}{2}} = 255$

Safety index

$$\beta = \frac{\overline{R} - \overline{Q}}{\sqrt{\sigma_R{}^2 + \sigma_Q{}^2}} = \frac{3734 - 2157.8}{\sqrt{373^2 + 255^2}} = 3.49$$

This $\beta$ value (3.49) is comparable to a design level safety target, - 3.5.

*Operating* level strength (working stress method)

In this case, $R_N = 1.33(807 + 807 + 218) = 2436$ k-ft

NOTE: $1.33 = \frac{1}{0.75}$ where 0.75 is the Operating level allowable stress factor.

Mean,
$$\overline{R} = 1.12(2436) = 2729$$

$$\sigma_R = (.10)(2729) = 273$$

Loads same as previous example,

$$\beta = \frac{\overline{R} - \overline{Q}}{\sqrt{\sigma_R{}^2 + \sigma_Q{}^2}} = \frac{2729 - 2157.8}{\sqrt{273^2 + 255^2}} = 1.53$$

NOTE: This value is too low; the AASHTO Guide Specification used 2.3 as a target for the operating level—the explanation is the relatively larger 75-year return period loading used in the AASHTO design LRFD calibration compared to evaluation.

For a typical live load used for evaluation—ref. 5 (NCHRP 301), used a mean load factor 1.50 which is appropriate for two-year intervals instead of 1.79 (75-year maximum design value). This leads to:

$$\overline{Q} = 807 + \left(\frac{1.50}{1.79}\right)(1228 + 122.8) = 1939$$

and

$$\sigma_Q = \left[80.7^2 + (1029 \times 0.18)^2 + (103 \times 0.8)^2\right]^{1/2} = 218.2$$

$$\beta = \frac{2729 - 1939}{\sqrt{273^2 + 218.2^2}} = 2.26$$

This $\beta$ value is similar to the acceptable target for evaluation at operating levels.

3.6.3 Derivation of Proof-Load Factors

Subsequent to a proof load, the following changes in data should be apparent.

Dead load—The bridge is known to carry whatever dead load is present. Therefore, $V_D = 0$.

Resistance—The test load capacity has been verified. So, corresponding to the level of load placed on the structure, the resistance uncertainty is zero, i.e., $V_R = 0$. A further question is whether the strength bias, i.e., the ratio of true mean to the nominal used in the strength equations, should be used. Typically, this bias ranges about 1.12. It is assumed herein that if the load test is stopped while behavior is still linear and no sign of initial distress has been observed, then the bias $B_R = 1.12$ can still be applied. If the test is stopped because the engineer feels the true strength has been reached, e.g., there is onset of nonlinear response or the appearance of distress, then the strength bias should be taken as 1.0. The effect of these differences will be seen in selection of the rating levels following the test.

Live Load—The future live loads are not known with any greater certainty following the test. However, a satisfactory performance during the test indicates that we should have no concern for any analysis uncertainty. That is, the loads will be carried in the future in the same distribution pattern in which the structure carried the proof loads. Therefore, the analysis portion of the load effect uncertainty should be removed. As cited above, eliminating analysis uncertainty reduces $V_L$ from 0.18 to 0.14.

Impact—There is no change in the assessment of the dynamic load allowance based on the AASHTO Design Code unless a moving load test is performed to investigate the impact.

3.6.4 Example 2—Test Has Been Performed

The safety indices will be shown for several levels of test magnitude.

1. Assume a successful load test has been carried out and the load has reached the nominal design strength moment (3334 k-ft) and no distress was observed.

   Using the database given in Example 1 and the parameters appropriate *after* a test, we obtain:

   Resistance, $\bar{R} = 1.12(3334) = 3734$; $\sigma_R = 0$

   Dead Load, $\bar{D} = 807$, $\sigma_D = 0$

   Live Load, $\bar{L} = 1228$, $\sigma_L = 0.14(1228) = 172$

   Impact, $\bar{I} = 122.8$, $\sigma_I = 98$ (same as before)

$$\beta = \frac{3734 - (807 + 1228 + 122.8)}{\sqrt{0 + \left(0^2 + 172^2 + 98^2\right)}} = 7.96 \text{ (very high)}$$

2. Assume test reaches the nominal operating loading moment (2436 k-ft) with no distress. Then:

   $\bar{R} = 1.12(2436) = 2729$, $\sigma_R = 0$

   and: $\bar{D} = 807$, $\sigma_D = 0$; $\bar{L} = 1228$, $\sigma_L = 172$; $\bar{I} = 122.8$, $\sigma_I = 98$

$$\beta = \frac{2729 - (807 + 1228 + 122.8)}{\sqrt{0 + \left(0^2 + 172^2 + 98^2\right)}} = 2.88$$

Thus, the proof test raises the calculated operating level safety index, $\beta$, from 1.53 (unacceptable) found in Example 1 to 2.88. As cited above, the acceptable target beta for operating level is given as 2.3.

## 3.7 TARGET PROOF-LOAD FACTORS

The next step is to select the load factors appropriate to a proof-test situation. The basis for the calibration model will be as follows:

Inspection Interval—2 years. This interval is appropriate to a rating level and is needed to select the statistical parameters of the load distribution. From Nowak's data, for a 2-year interval, the mean expected maximum load level for two lanes simultaneously loaded is 0.85 x 1.65 x the HS20 load effect.

Traffic Intensity—The load data just cited were developed from sites with heavy traffic volumes and overloaded vehicles.

Bridge Type—It will be assumed that the operating level load factor will be the reference level for calibration. The bridge will be assumed as a redundant structure without fracture critical details, for which most states would accept operating levels as their target safety requirements. Based on NCHRP Report 301 and the corresponding AASHTO Guide Specification that came from that project, a target safety index of about 2.3 was associated with operating levels.

Proof Test—It is assumed that the performance during the test is acceptable and the full load is applied without signs of distress. Further, it is assumed that the test loadings fully envelop all the limit state conditions that need to be considered in the analysis. For convenience, the loadings will be represented in terms of HS20 levels.

Let $X_p$—Proof load test factor

If the test is stopped prior to any visible distress, then the nominal resistance, $R_n$, is:

$$R_n = X_p + D$$

since the dead load is also being supported. The expression for safety index becomes:

$$\beta = \frac{1.12\left[X_p L_{HS20}\left(1 + I_{AASHTO}\right) + \overline{D}\right] - \left[\overline{D} + \overline{L} + \overline{I}\right]}{\sqrt{\sigma_R^2 + \sigma_D^2 + \sigma_L^2 + \sigma_I^2}}$$

in which the terms are as defined above. Using the same data as in the above example with a two-year interval on mean live load (i.e. 1.65 x 0.85 x HS20 or 1132 k-ft) gives:

$$\beta = \frac{1.12X_P(807)(1.27) - [1132 + 113.2] + 0.12(807)}{\sqrt{0.14^2(1132)^2 + 0.8^2(113.2)^2}}$$

$$\beta = \frac{X_P(1148) - 1245 + 97}{182}$$

which results in the following table:

| $X_P$ | β |
|---|---|
| 1.2 | 1.26 |
| 1.3 | 1.89 |
| 1.4 | 2.57 |
| 1.5 | 3.15 |
| 1.6 | 3.78 |

Rounding off to the nearest 0.1, it appears that a factor of $X_p = 1.4$ would be consistent with the target safety index. This value is not surprising since the load factor is 1.3 in LFD and 1.33 in working stress method. The factor needs to be slightly higher because only the live load is factored during the proof test. The dead load is assumed to be the mean value. In calculating a rating using the working stress method, the strength must be 1.33 x the sum of dead and live load effects. In the proof test the total applied load is now 1.4 x live load plus 1.0 x dead load. However, the test reduces some of the uncertainty which allows a lower overall proof-load capacity than the 1.33 x (dead plus live) implied in the nominal rating calculations.

The 1.4 factor was derived above for the specific example of a 60-ft span. However, it does provide adequate safety for other spans. For example, for a very short span the impact is 1.3 and the dead load may be neglected. The above equations then give for beta, for a proof-load factor of 1.4:

$$\beta = \frac{1.12\, X_p\, L_{AASHTO}(1 + 0.3) - 1.65 \times 0.85 \times L_{AASHTO}(1.1)}{L_{AASHTO}\left(0.14^2 + 0.8^2 + 0.1^2\right)^{1/2}}$$

$$= 3.07$$

Similarly, for a long span, the impact factor drops off and the dead load quantity increases. This leads to a smaller value for beta, for a D/L value of 3.0:

$$\beta = \frac{1.12 X_p L_{AASHTO}(1.0) - 1.65 \times 0.85 \times L_{AASHTO}(1.1) + 0.12 D}{L_{AASHTO}(0.14^2 + 0.8^2 + 0.1^2)^{1/2}}$$

$$= 2.39$$

Thus, the selected value of 1.4 provides acceptable levels of beta over the full range of application. The lack of a uniform beta, i.e., higher values for shorter spans than for longer spans, may be offset somewhat by the fact that shorter spans are likely to have higher load biases (compared to HS20) than longer spans. These differences are not reflected in the data above.

In summary, the suggested proof-test load factor is 1.4 for the reference case described above. Adjustments of this factor are discussed in the next section to account for situations which differ from the base case.

## 3.8 ADJUSTMENTS IN PROOF-TEST LOAD FACTOR

This section describes the adjustments in proof-load factor needed to account for a variety of situations. The adjustments are reflected in the values given in Section 7 of the proposed Manual.

1. Observed Distress During the Test

   The resistance bias described above should not be used if the test is stopped due to observed distress prior to full application of the proof-test load. To account for this situation, the required proof-test factor $X_p$ should be increased by the factor of 1.12. The influence of this change will be seen in the calculated operating rating factor which is given in Eqn. 7-2 of the proposed Manual. The observed distress indicates the true resistance has been reached and should be used for the rating calculation. When no distress is observed, the final observed resisance is taken as a nominal resistance which typically is a safe conservative value and is exceeded by the true capacity by at least 12%.

2. One-Lane Controls

   One purpose of the proof-test load factor is to envelop the future extreme bridge loads. The data above showed that for a typical two-lane bridge the expected maximum load in each lane was 0.85 times the expected maximum single-lane value. An adjustment in $X_p$ is needed if we have either: a one-lane structure or some component of a multi-lane structure which due to its distribution factors shows greater load effects from a single-lane loading than from the two-lane loadings which are reduced by 0.85. In this case, the proof-test should be performed with a factor $X_p$ of 1.4 on two lanes loaded, and a factor of $X_p$ of 1.4 x 1.15 = 1.61 on a single-lane load.

3. Infrequent Inspections

   If inspections are expected to be infrequent, then the live loading to be enveloped by $X_p$ should correspond to a period longer than two years. The difference in expected maximum loading between two years and a full lifetime is given above as 1.65 vs. 1.79 about a 10% difference. Since infrequent inspection may imply that corrective maintenance will also not be undertaken, then it is prudent to increase the recommended proof-load factors by 10%.

4. Non-Redundant Structures

   The target beta of 2.3 is associated with operating levels and is deemed acceptable for redundant spans with reserve strength to provide greater safety against collapse. For non-redundant spans, a target beta of 3.5, corresponding to inventory or design levels is needed. From the table above, to increase beta by 1.0 requires a 10% increase in $X_p$. A double penalty, such as applying this additional 10% and also using the lower inventory level for posting, is not warranted.

5. Additional Factors

   Further adjustments in $X_p$ may be made using the material in Reference 6. The variables discussed therein include traffic intensity and quality of maintenance and data are provided for further adjustments in $X_p$.

## REFERENCES


1. Agarwal, A. C. and Selvadurai, A.P.S. 1991. "Behavior of Shear Connection Between Steel Girder and Concrete Deck Slab." Proceedings, CSCE Annual Conference, Vol. 3.

2. Bakht, B. and Jaeger, L. G. 1992. "Ultimate Load Test of Slab-on-Girder Bridge." ASCE Journal of Structural Engineering, Vol. 118, No. 6, pp. 1608-1624.

3. Jaeger, L. G. and Bakht, B. 1988. *Bridge Analysis by Microcomputer*. McGraw Hill, New York.

4. Mahue, J. and Agarwal, A.C. 1992. *Test on the 12th Brant Bridge.* Structures Research Report. Ministry of Transportation of Ontario. In preparation.

5. Moses, F. and Verma, D. 1987. "Load Capacity Evaluation of Existing Bridges." NCHRP Report 301, Transportation Research Board, National Research Council.

6. AASHTO 1989. "Guide Specifications for Strength Evaluation of Existing Steel and Concrete Bridges," Washington, D.C.

7. Burdette, E. G. and Goodpasture, D. W., "Correlation of Bridge Load Capacity Estimates with Test Data," NCHRP Report 306, June 1988.

8. Pinjarkar, S. G., et al, "Nondestructive Load Testing for Bridge Evaluation and Rating," Final Report, NCHRP Project 12-28(13), Feb. 1990.


## ACKNOWLEDGMENTS


The research performed herein was done under NCHRP Project 12-28(13)A by A. G. Lichtenstein and Associates. Major contributions were made by project Subconsultants Fred Moses, Chairman of the Department of Civil Engineering at the University of Pittsburgh and Baidar Bakht of the Ministry of Transportation, Ontario. L. G. Jaeger's help in the development of the analytical treatment in Chapter 2 is gratefully acknowledged.